Sensors & Transducers, Vol. 258, Issue 4, July 2022, pp. 31-35

Sensors & Transducers
Published by IFSA Publishing, S. L., 2022
http://www.sensorsportal.com

Propagation of Azimuthally Polarized Bessel-Gaussian Beam through Helical Axicon

[1] Ibrahim G. H. LOQMAN, [1, *] Abdu A. ALKELLY and [1, 2] Hassan T. ALAHSAB

[1] Physics Department, Faculty of Science, Sana'a University, Sana'a, Yemen
[2] Physics Department, Faculty of Applied Science, Dhamar University, Dhamar, Yemen
[*] Tel.: +967777267057
E-mail: a.alkelly@su.edu.ye

Received: 1 June 2022 /Accepted: 5 July 2022 /Published: 29 July 2022

Abstract: Propagation properties of azimuthally polarized Bessel-Gaussian (APBG) beams with non-zero order through a helical axicon (HA) are theoretically investigated. The formula of APBG beams field in the focal region are derived by the vector diffraction theory. Numerical results illustrate that the beam and axicon parameters affect the intensity distribution in the focal region very considerably. Super--long transversely polarized focal depth with different shapes are obtained by choosing appropriate values of parameters. We also observed that a focal shift occurs which depends on both axicon parameter and numerical aperture. We expect that focusing APBG beams by HA can be used in optical trapping.

Keywords: Bessel-Gaussian beam, Azimuthal polarization, Helical axicon, Vector di□raction theory.

1. Introduction

A helical axicon is a hybrid of a spiral phase plate, that is an optical element whose thickness increases azimuthally, and of an axicon [1]. It has attracted researchers' interest due to its unique characteristics and different applications. It is shown that the helical axicon (HA) can be used to transform Gaussian beam and a plane wave into a vortex beam [2, 3]. The HA also has been used to generate Bessel-Gaussian beams of arbitrary order [4], spiraling Bessel beams with adjustable topological charges from Laguerre-Gaussian beam [5], vortex beams [6, 7] and non-di□racting Bessel beam by conversion high-order Laguerre-Gaussian beam [8]. It is found that the topological charge and axicon parameter can alter the focal pattern in the focal region [9, 10]. A general approximate analytical expressions of the Fresnel diffraction of Laguerre–Bessel–Gaussian beam by the HA has been derived analytically based on the stationary phase method [11].

Last decades, high order Bessel–Gaussian beams that propagate with stability in both size and intensity have attracted lots of researchers' attentions due to their extraordinary properties. Such class of beams propagate without divergence, carrying orbital angular momentum with a helical phase fronts and have the property of self-healing [12 - 15]. These properties have propitiated their application in optical trapping [16, 17], optics communication [18] and generating perfect optical vortices [19]. Recently, focusing of polarized Bessel-Gaussian beams which have either pure azimuthal or pure radial polarization had been studied extensively. A needle of strong longitudinal polarized field with long depth of focus and strong intensity has been obtained by focusing a radially polarized Bessel–Gaussian beams with a high numerical aperture lens and a diffractive optical element [20]. In [21], X. Gao et. al. have investigated focusing properties of Bessel–Gaussian beam with radial varying polarization detail. The same group, also, studied the focus shaping of the radially polarized Bessel–Gaussian beam with a sine-azimuthal variation wave front [22]. Multiple intensity rings, dark hollow have been generated by focusing radial varying polarized Bessel–Gaussian beam with radial phase modulation [14]. It is found that radially polarized laser beams have small focuses and non-propagating longitudinal field components; while azimuthally polarized beams have hollow intensity distributions form [17].

By taking into account the fact that focusing Bessel–Gaussian beams are very important in many applications such as optical trapping [17] and the properties of the HA. To the best of our knowledge, the propagation properties of APBG beam through the HA are investigated for the first time in this work. The propagation properties of focused APBG beams such as depth of focus (DOF) and the full width at half maximum (FWHM) by a linear axicon, that is a special case of the HA when the topological charge of a HA p = 0, are also studied. The theoretical model is introduced in section 2. The numerical results are discussed in section 3. In section 4 the conclusion of results is shown.

2. Theoretical Model

The electric field of the APBG beam $E(\rho, \phi)$, in cylinderical coordinate system (ρ, ϕ, z), at the source plane can be given by

$$\boldsymbol{E}(\rho, \phi) = E(\rho, \phi)\boldsymbol{e_{\phi}}, \quad (1)$$

where $\boldsymbol{e_{\phi}}$ is the azimuthal unit vector of the polarized direction and $E(\rho, \phi)$ is the electric field of Bessel-Gaussian beam that is given by [23]

$$E(\rho, \phi) = J_1(\beta\rho)\exp\left(-\frac{\rho^2}{w_0^2}\right)\exp(i\phi), \quad (2)$$

where J_1 is the Bessel function of the first kind of order 1 which is the topological charge of the optical vortex, β is the transverse wave number that indicates the quickness of the fluctuation of Bessel function and w_0 is the beam width. The transmittance of the HA is defined as [6]

$$T = \exp(\mathrm{i}\alpha\rho + ip\phi), \quad (3)$$

where α is the axicon parameter that shows the axicon strength and $p = 0, \pm 1, \pm 2, \ldots$ is a topological charge of the HA. Based on the variable transformation Eq.3 can be rewritten as [9, 10]:

$$T = \exp\left[i\alpha\rho_b\frac{\rho}{\rho_b} + \mathrm{i}p\phi\right] = \exp\left[i\alpha\rho_b\frac{\rho}{\rho_b} + ip\phi\right] = \exp\left[i\eta\frac{\sin\theta}{NA} + ip\phi\right], \quad (4)$$

where $\eta = \alpha\rho_b$ is the dimensionless axicon parameter, NA is the numerical aperture and θ is the tangential angle with respect to the optical axis as shown in Fig. 1.

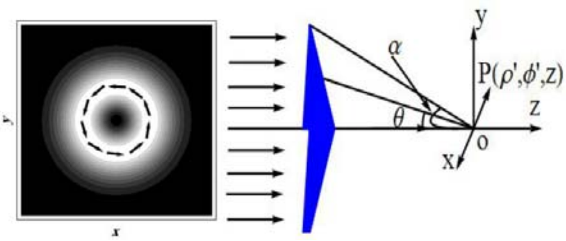

Fig. 1. Scheme for a azimuthally polarized Bessel-Gaussian beam focused by helical axicon.

According to vector diffraction theory, the electric field of APBG beam focused by HA is [24, 25]:

$$\boldsymbol{E}(\rho', \phi', z) = E_{\rho'}\boldsymbol{e_{\rho'}} + E_{\phi'}\boldsymbol{e_{\phi'}} + E_z\boldsymbol{e_z}, \quad (5)$$

where $\boldsymbol{e_{\rho'}}, \boldsymbol{e_{\phi'}}$ and $\boldsymbol{e_z}$ are the radial, azimuthal, and longitudinal unit vectors, respectively. The amplitudes of the three orthogonal components $E_{\rho'}, E_{\phi'}$ and E_z in the focal region are given by

$$\begin{pmatrix} E_{\rho'}(\rho', \phi', z) \\ E_{\phi'}(\rho', \phi', z) \\ E_z(\rho', \phi', z) \end{pmatrix} = -\frac{iA}{\pi}\int_0^{\alpha}\int_0^{2\pi}\sqrt{\cos\theta} * E(\theta, \phi)T(\theta, \phi)\exp[ik(z\cos\theta + \rho'\sin\theta * \cos(\phi - \phi'))] \begin{pmatrix} -\sin\theta\sin(\phi - \phi') \\ \sin\theta\cos(\phi - \phi') \\ 0 \end{pmatrix} d\phi d\theta, \quad (6)$$

where k is the wave number, $\alpha = \arcsin(\mathrm{NA})$ is the convergence angle corresponding to the radius of the incident optical aperture. The coordinate system is shown in Fig. 1. In order to simplify calculation process, Eq.2 can be expressed as [26, 27]

$$E(\theta, \phi, 0) = J_1\left(\frac{2\beta_1\sin\theta}{NA}\right)\exp\left[-\left(\frac{\beta_2\sin\theta}{NA}\right)^2\right]\exp(i\phi), * \cos(\phi - \phi'))] \quad (7)$$

where β_1 and β_2 are the ratios of pupil diameter to the beam diameter.

By substituting Eqs. (4) and (7) into Eq. (6) the three orthogonal component of electric field can be obtained as

$$\begin{pmatrix} E_{\rho'}(\rho',\phi',z) \\ E_{\phi'}(\rho',\phi',z) \\ E_z(\rho',\phi',z) \end{pmatrix} = -\frac{iA}{\pi}\int_0^{\alpha}\int_0^{2\pi}\sqrt{\cos\theta}$$
$$* \exp\left[-\left(\frac{\beta_2 \sin\theta}{NA}\right)^2\right] J_1\left(\frac{2\beta_1 \sin\theta}{NA}\right) \exp\left[i\eta\frac{\sin\theta}{NA}\right.$$
$$\left. + \exp(i(+1)\varphi)\right] \exp[ik(\rho'\sin\theta\cos(\phi-\phi'))]$$
$$\begin{pmatrix} -\sin\theta\sin(\phi-\phi') \\ \sin\theta\cos(\phi-\phi') \\ 0 \end{pmatrix} \exp[ikz\cos\theta]d\phi d\theta. \quad (8)$$

The integration with respect to φ can be accomplished by using the following formula:

$$\int_0^{2\pi} \sin(\phi-\phi')\exp[im\phi + it\cos(\phi-\phi')]d\phi$$
$$= \pi i^m \exp(im\phi')[J_{m+1}(t) + J_{m-1}(t)], \quad (9)$$

and

$$\int_0^{2\pi} \cos(\phi-\phi')\exp[im\phi + it\cos(\phi-\phi')]d\phi$$
$$= \pi i^{m+1} \exp(im\phi')[J_{m+1}(t) - J_{m-1}(t)]. \quad (10)$$

Therefore, the orthogonal components of the output electric field are given by:

$$\begin{pmatrix} E_{\rho'}(\rho',\phi',z) \\ E_{\phi'}(\rho',\phi',z) \\ E_z(\rho',\phi',z) \end{pmatrix} = i^p A\exp(i(p+1)\phi')$$
$$* \int_0^{\alpha}\sqrt{\cos\theta}J_1\left(\frac{2\beta_1\sin\theta}{NA}\right)\exp\left[-\left(\frac{\beta_2\sin\theta}{NA}\right)^2 + i\eta\frac{\sin\theta}{NA} + \right.$$
$$\left. ikz\cos\theta\right] \begin{pmatrix} -\sin\theta[J_{p+2}(k\rho'\sin\theta) + J_p(k\rho'\sin\theta)] \\ i\sin\theta[J_{p+2}(k\rho'\sin\theta) - J_p(k\rho'\sin\theta)] \\ 0 \end{pmatrix} d\theta. \quad (11)$$

The optical intensity is proportional to the modulus square of Eq. 5.

3. Numerical Calculation and Discussion

In this section some numerical calculation will be carried out in order to obtain the properties of propagation APBG beam through helical axicon depending on Eq. 11. It is noticeable that the integral over the parameter θ could not accomplished analytically; therefore, the numerical integration will be used. In our calculation, we consider A equal unit one and $\lambda = 632.8$nm and the distance unit in figures in this work is the wavelength of the incident beam in vacuum.

Fig. 2 illustrates the intensity distribution of APBG beam with HA for different axicon parameter $\eta = 0, \eta = 2, \eta = 4, \eta = 6, \eta = -2$ and $\eta = -4$ under condition of $\beta_1 = 2$, $\beta_2 = 1$, $p = 1$, and $NA = 0.95$. This figure shows that the intensity distribution vary with respect to axicon parameter. It is clearly shown that the focal hole shape still constant as the axicon parameter changed and the intensity distribution is symmetry about the z axis. For $\eta = 0$ as it is shown in Fig. 2 (a) the focal region is symmetry about z and its center is at $z = 0$. In addition, it can be seen from Fig. 2 (b-d) the generated focal hole region shifts away from the HA on increasing the positive value of the axicon parameter η. In the other hand, the generated focal hole in the focal region shifts toward the HA on decreasing the negative value the axicon parameter as it is shown in Fig. 2 (e and f) that are for $\eta = -2$ and $\eta = -4$, that indicate focal shift phenomenon occurs that means the movement of the center of focal hole. It can be concluded that different HA different focal hole regions for the same incident beam.

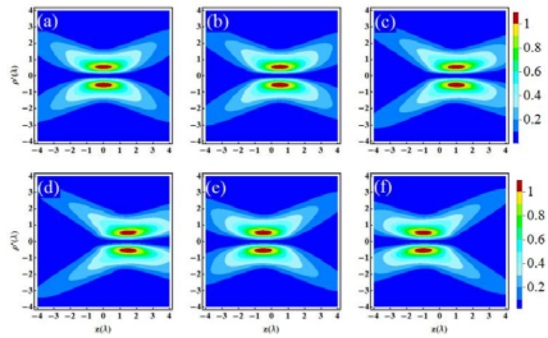

Fig. 2. Intensity distribution of APBG beam with HA under condition $\beta_1 = 2$, $\beta_2 = 1$, $p = 1$, $NA = 0.95$ and (a) $\eta = 0$, (b) $\eta = 2$, (c) $\eta = 4$, (d) $\eta = 6$, (e) $\eta = -2$, (f) $\eta = -4$, respectively.

Fig. 3 exhibits the intensity distribution of APBG beam with a HA for positive and negative different values of topological charge under condition of $\eta = 4$, $\beta_1 = 2$, $\beta_2 = 1$, and $NA = 0.95$. It is shown from Fig. 3 (a and f) that the focused APBGB with $p = 0$ and -2 are not hollow and have peaks on the optical axes due to the presence of J_0 that is found in the integrand for both $p = 0$ and -2. In the other hand, the focal hole region is constructed for $p \neq 0$ and -2 as can be seen in Fig. 3(b, c, d and e). The radius of the focal hole increases as the topological charge either positively increase or negatively decrease. By comparing Fig. 3 (b with e) and Fig. 3 (d with g) it is found that the focal hole region is longer and have smaller radius for negative values of p than positive values. It can be conclude that the HA changes the topological charge of the incident beams and convert it to a non-vortex beam [8, 7].

Now, let the parameters β_1 and β_2 vary to show how the focal hole region change. In Fig. 4 the parameter β_1 increase from 1 to 3.5 for $\beta_2 = 1$ and in Fig. 4 the parameter β_2 increase from 1.5 to 2.5 for $\beta_1 = 3$ the other parameters are $\eta = 2$, $NA = 0.95$, and $p = 1$ for both of them. It is obviously shown that the shape of the focal hole region in these two figures have changed considerably and some novel focal hole patterns are appear including dark hollow focus, multiple intensity ring that can be used to construct optical traps. In addition, the focal hole region shift is not related to the parameters β_1 and β_2 as it is shown from Figs. 4 and 5. In addition, the position of the maximum intensity value change as the values of both parameters β_1 and β_2 change with forming different focal region shapes. Therefore, they can affect the focal pattern considerably and produce some novel focal hole regions that can be used in optical trapping.

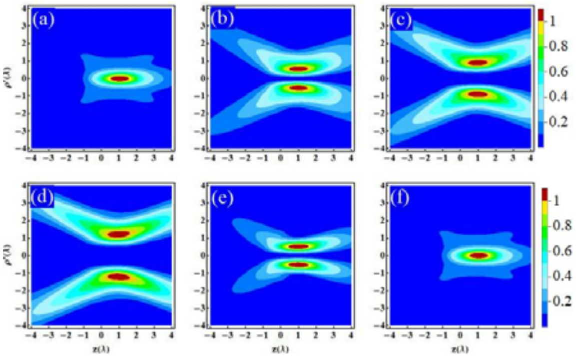

Fig. 3. Intensity distribution of APBG beam with HA under condition $\beta_1 = 2, \beta_2 = 1, \eta = 4, NA = 0.95$ and (a) $p = 0$, (b) $p = 1$, (c) $p = 2$, (d)$p = 3$, (e) $p = -1$ and (f) $p = -2$, respectively.

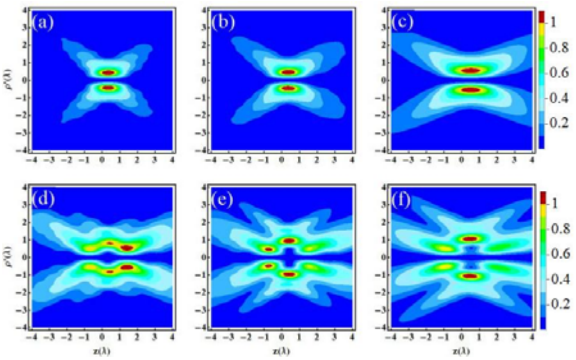

Fig. 4. Intensity distribution of APBG beam with HA under condition $\eta = 2$, $NA = 0.95$, $p = 1$,$\beta_2 = 1$ and (a) $\beta_1 = 1$, (b) $\beta_1 = 1.5$, (c) $\beta_1 = 2$, (d) $\beta_1 = 2.5$, (e)$\beta_1 = 3$, (f) $\beta_1 = 3.5$, respectively.

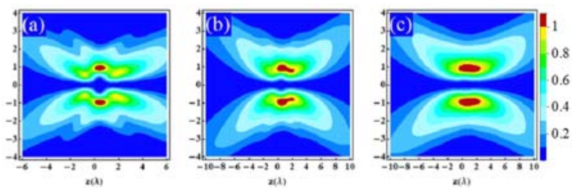

Fig. 5. Intensity distribution of APBG beam with HA under condition $\eta = 4$, $NA = 0.95$ $\beta_1 = 3$ and (a) $\beta_2 = 1.5$, (b) $\beta_2 = 2$, (c) $\beta_2 = 2.5$, respectively.

The intensity distribution of APBG beams with different values of numerical aperture with $p = 1$ and $p = 0$, that is corresponding to a linear axicon, under condition $\eta = 2$, $\beta_1 = 3$ and $\beta_2 = 3$ are shown in Fig. 6. It can be seen that the intensity distribution in the focal region strongly depend on both the nume rical aperture and the topological charge. While a transversely polarized focal hole is formed with $p = 1$ an extended focal spot is formed with $p = 0$. The focal depth considerably extend as the numerical aperture decrease and the focal shift increase, also, that are coincide with our previous work [28]. A super–long focal tube is obtained from focusing APBG beams with small values of numerical aperture. The dependence of both DOF and FWHM of focused APBG beam by a linear axicon on the numerical aperture are illustrated in Fig. 7 under condition of $\eta = 2$, $\beta_1 = 3$, $\beta_2 = 3$, and $NA = 0.95$. It is clearly shown that the depth of focus increases considerably as the NA decreases. The depth of focus equal 48.9λ and 38.6λ for $NA = 0.40$ and $NA = 0.45$, respectively. Moreover, the FWHM is also extend as the numerical aperture decrease.

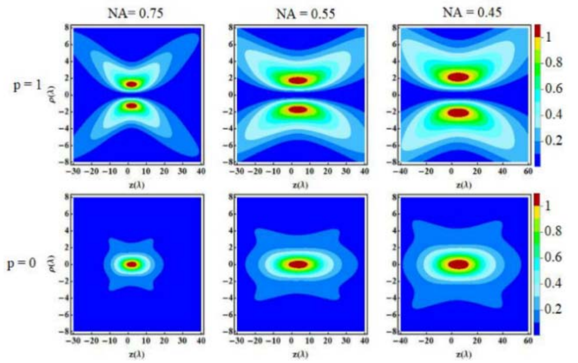

Fig. 6. Intensity distribution of APBG beam with HA under condition $\eta = 2$, $\beta_1 = 3$ and $\beta_2 = 3$ with $p = 0$ and $p = 1$.

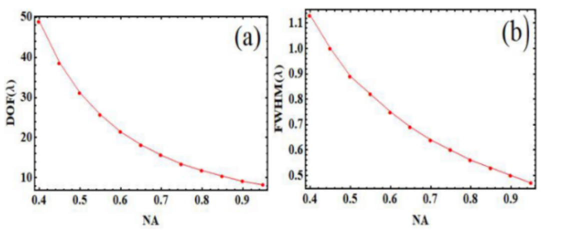

Fig. 7. Depth of focus (DOF) and the full width at half maximum (FWHM) of a focused APBG beam with HA under condition $\eta = 2$, $\beta_1 = 3$, $\beta_2 = 3$ and $p = 0$ that is corresponding to a linear axicon.

4. Conclusions

In summary, by using the vector diffraction theory propagation properties of the azimuthally polarized Bessel-Gaussian beam (APBGB) through helical axicon is numerically investigated. Our numerical results clearly show that the intensity distribution in the focal region of the APBGB can be adjusted considerably by axicon parameter, topological charge of the spiral phase, and beam parameters. A long focal tube has been obtained. We suggest that focusing of APBGB by HA may find application in optical trapping.

References

[1]. S. Khonina, V. Kotlyar, V. Soifer, M. Shinkaryev, G. Uspleniev. Trochoson, *Optics Communications,* Vol. 91, 1992, pp. 158–162.

[2]. V. V. Kotlyar, A. A. Kovalev, R. V. Skidanov, O. Y. Moiseev, V. A. Soifer, Di□raction of a finite-radius plane wave and a gaussian beam by a helical axicon and a spiral phase plate, *J. Opt. Soc. Am. A*, Vol. 24, Issue 7, 2007, pp. 1955–1964.

[3]. M. Beijersbergen, R. Coerwinkel, M. Kristensen, J. Woerdman, Helical-wavefront laser beams produced with a spiral phaseplate, *Optics Communications,* Vol. 112, 1994, pp. 321–327.

[4]. V. Arriz´on, U. Ruiz, D. Aguirre-Olivas, D. S´anchez-de-la Llave, A. S. Ostrovsky, Comparing e□ciency and accuracy of the kinoform and the helical axicon as bessel–gauss beam generators, *J. Opt. Soc. Am. A*, Vol. 31, Issue 3, 2014, pp. 487–492.

[5]. S. Qiong-Ge, Z. Ke-Ya, F. Guang-Yu, L. Zheng-Jun, L. Shu-Tian, Generalization and propagation of spiraling Bessel beams with a helical axicon, *Chinese Physics B,* Vol. 21, Issue 1, 2012, p. 014208.

[6]. V. Kotlyar, A. Kovalev, V. Soifer, C. S. Tuvey, J. A. Davis, Sidelobe contrast reduction for optical vortex beams using a helical axicon, *Optics Letters*, Vol. 32, Issue 8, 2007, pp. 921–923.

[7]. S. Topuzoski, L. Janicijevic, Diffraction of laguerre-gaussian beam by a helical axicon, *Acta Physica Polonica-Series A General Physics,* Vol. 9, Issue 4, 2009, pp. 557.

[8]. S. Topuzoski, L. Janicijevic, Conversion of high-order Laguerre–Gaussian beams into Bessel beams of increased, reduced or zeroth order by use of a helical axicon, *Optics Communications,* Vol. 282, Issue 17, 2009, pp. 3426–3432.

[9]. X. Dong, T. Geng, S. Zhuang, Focusing properties of hyperbolic-cosine-Gaussian beams combining a helical axicon, *Optik,* Vol. 124, Issue 18, 2013, pp. 3422–3426.

[10]. G. Wang, Y. Miao, Q. Zhan, G. Sui, R. Zhang, Focusing of linearly polarized Lorentz-Gaussian beam with helical axicon, *Optik,* Vol. 130, Issue 2017, pp. 266–272.

[11]. F. Saad, Z. Hricha, M. Khouilid, A. Belafhal, A theoretical study of the Fresnel diffraction of Laguerre-Bessel-Gaussian beam by a helical axicon, *Optik,* Vol. 149, 2017, pp. 416–422.

[12]. S. Vyas, Y. Kozawa, S. Sato, Self-healing of tightly focused scalar and vector Bessel–Gauss beams at the focal plane, *J. Opt. Soc. Am. A,* Vol. 28, Issue 5, 2011, pp. 837–843.

[13]. S. Zhao, W. Zhang, L. Wang, W. Li, L. Gong, W. Cheng, H. Chen, J. Gruska, Propagation and self-healing properties of Bessel-Gaussian beam carrying orbital angular momentum in an underwater environment, *Scientific Reports,* Vol. 9, Issue 1, 2019, pp. 1–8.

[14]. B. Wu, X. Zeng, Y. Miao, Y. Fan, X. Gao, S. Zhuang, Focal shift of radial varying polarized Bessel-Gauss beam with radial phase modulation, *Optik,* Vol. 157, 2018, pp. 675–683.

[15]. G. Wu, F. Wang, Y. Cai, Generation and self-healing of a radially polarized Bessel-Gauss beam, *Physical Review A,* Vol. 89, Issue 4, 2014, pp. 043807.

[16]. G. Volpe, G. P. Singh, D. Petrov, Optical tweezers with cylindrical vector beams produced by optical fibers, in: Optical Trapping and Optical Micromanipulation, *International Society for Optics and Photonics*, Vol. 5514, 2004, pp. 283–292.

[17]. F. Wu, B. Zhang, Z. Liu, Y. Tang, N. Zhang, Optical trapping forces of a focused azimuthally polarized Bessel-Gaussian beam on a double-layered sphere, *Optics Communications,* Vol. 405, 2017, pp. 96–100.

[18]. F. Zhu, S. Huang, W. Shao, J. Zhang, M. Chen, W. Zhang, J. Zeng, Free-space optical communication link using perfect vortex beams carrying orbital angular momentum (oam), *Optics Communications,* Vol. 396, 2017, pp. 50–57.

[19]. M. K. Karahroudi, B. Parmoon, M. Qasemi, A. Mobashery, H. Saghafifar, Generation of perfect optical vortices using a Bessel–Gaussian beam diffracted by curved fork grating, *Applied Optics,* Vol. 56, Issue 21, 2017, pp. 5817–5823.

[20]. K. Huang, P. Shi, X.-l. Kang, X. Zhang, Y.-P. Li, Design of doe for generating a needle of a strong longitudinally polarized field, *Optics Letters,* Vol. 35, Issue 7, 2010, pp. 965–967.

[21]. X. Gao, R. Fu, H. Shen, X. Dong, T. Geng, S. Zhuang, Focus shaping of Bessel–Gauss beam with radial varying polarization, *Optica Applicata,* Vol. 42, Issue 3, 2012, pp. 481–491.

[22]. X. Gao, D. Zhang, T. Mei, R. Fu, S. Zhuang, Focus shaping of the radially polarized Bessel–Gauss beam with a sine-azimuthal variation wavefront, *Optica Applicata,* Vol. 43, Issue 3, 2013, pp. 567-582.

[23]. F. Gori, G. Guattari, C. Padovani, Bessel-Gauss beams, *Optics Communications,* Vol. 64, Issue 6, 1987, pp. 491–495.

[24]. K. S. Youngworth, T. G. Brown, Focusing of high numerical aperture cylindrical-vector beams, *Optics Express,* Vol. 7, Issue 2, 2000, pp. 77–87.

[25]. S. Sato, Y. Kozawa, Hollow vortex beams, *J. Opt. Soc. Am. A,* Vol. 26, Issue 1, 2009, pp. 142–146.

[26]. E. Y. Yew, C. J. Sheppard, Tight focusing of radially polarized Gaussian and Bessel-Gauss beams, *Optics Letters,* Vol. 32, Issue 23, 2007, pp. 3417–3419.

[27]. X. Gao, S. Hu, J.-S. Li, Z.-H. Ding, H.-M. Guo, S.-L. Zhuang, et al., Tunable optical gradient trap by radial varying polarization Bessel–Gauss beam, *Journal of Biomedical Science and Engineering,* Vol. 3, Issue 3, 2010, pp. 304–307.

[28]. A. A. Alkelly, I. G. H. Loqman, H.-M. H. T. Al-Ahsab, Focus shaping of cylindrically polarized vortex beams by a linear axicon, *Electronic Journal of University of Aden for Basic and Applied Sciences,* Vol. 2, Issue 4, 2021, pp. 145–150.